MODELING THE VNIR REFLECTANCE OF GEOMETRICALLY COMPLEX SPACE WEATHERED GRAINS WITH THE MULTIPLE SPHERE T-MATRIX MODEL C. Legett IV[1], T. D. Glotch[1], and P. G. Lucey[2], [1]Stony Brook University, 255 Earth and Space Sciences Building, Stony Brook, NY 11794-2100, carey.legett@stonybrook.edu, [2]Hawaii Institute of Geophysics and Planetology, University of Hawaii.

Introduction: Space weathering can be defined as the gradual changes experienced by the surfaces of airless planetary bodies due to exposure to the vacuum of space, radiation, and micrometeoroid bombardment [1]. Characteristic visible and near infrared (VNIR) spectral changes due to space weathering include a decrease in albedo and a general "reddening" of spectra (increasing reflectance with increasing wavelength). Apollo-returned lunar soils contain grains with amorphous rims with nanophase metallic iron ($npFe^0$) particles dispersed throughout. Absorbing particles of this scale (10s of nm) have disproportionately large optical effects compared to their abundance. The size of the $npFe^0$ particles determines the amount of reddening observed -- smaller particles are associated with redder spectra in the VNIR than larger particles. A transition occurs at a particle size of about 30-50 nm, above which the spectra darken without reddening. Previous modeling work has failed to robustly reproduce this transition at the observed iron particle size, instead requiring larger than expected iron particles [2].

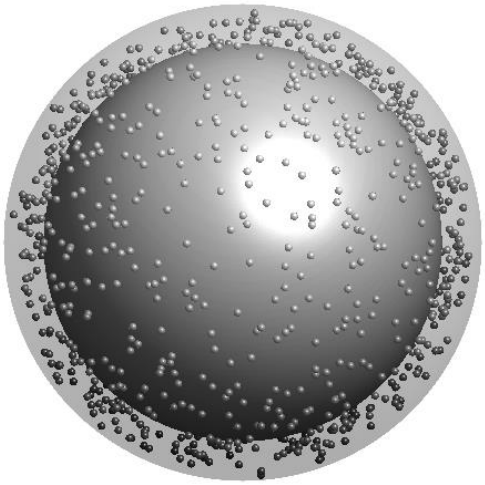

Figure 1. Representative modeled 3D grain showing a 1 µm host grain, 100 nm thick rim, with 1000 20 nm diameter iron particles dispersed throughout the rim. In this representation, the host grain and iron particles are rendered as opaque while the rim is translucent.

In this work, we simulate space weathered particles using the Multiple Sphere T-Matrix Model (MSTM) [3] to attempt to improve upon the successes of previous Mie-Hapke models and to resolve the $npFe^0$ grain size discrepancies. This approach improves on modeling approaches that rely on the use of effective medium approximations (EMAs) due to the loss of information inherent in simplifying the particles to spheres or coated spheres. Due to the high refractive index contrast between the rim and the $npFe^0$ inclusions, EMAs will only provide suitable effective optical constants for runs with very small inclusion size parameters and relatively low inclusion particle counts [4].

Methods: We construct particles as spheres of olivine (referred to as the host) with a thin, even rim of amorphous silica glass surrounding it (Figure 1). Within the rim but outside the host grain, we randomly populate a large number of identically sized $npFe^0$ particles. In the figure, we render the host grain as opaque and the rim translucent. We then construct particles with different $npFe^0$ sizes and abundances. Each component sphere requires the input of the radius, x, y, and z coordinates of the center, and optical constants n and k. The scattering and extinction efficiencies (Q_{sca} and Q_{ext}) output by MSTM are used to calculate the single scattering albedo:

$$\varpi = \frac{Q_{sca}}{Q_{ext}}$$

Then the scattering cross section (C_{sca}) and differential scattering cross section ($\frac{dC_{sca}}{d\Omega}$) are calculated (after [5]:

$$C_{sca} = Q_{sca} \cdot G$$

$$\frac{dC_{Sca}}{d\Omega} = \frac{S_{11}}{k^2}$$

Where G is the geometric cross section of the particle ($G = \pi r\text{^}2$), S_{11} is one of the scattering parameters output by MSTM, and k is the wavenumber of the light being scattered, at an angle of 150° (where 0° is the forward scattering direction).

From this, a phase function, *p*, is calculated:

$$p = 4\pi \frac{1}{C_{sca}} \frac{dC_{sca}}{d\Omega}$$

Which is then input to Hapke's bidirectional reflectance function (as P(g))[6]:

$$r(i,e,g) = \frac{\varpi}{4\pi}\frac{\mu_0}{\mu_0+\mu}\left[\left(1+B(g)\right)P(g) + H(\mu_0)H(\mu) - 1\right]$$

Where *i*, *e*, and *g* are the incident angle (0º), emergence angle (30º, equivalent to 150º above, but here 0º is the backscattering direction), and phase angle (difference in *i* and *e*, 30º). μ_0 and μ are the cosines of *i* and *e* respectively, and H is an approximation of the Ambartsumian-Chandrasekhar H function [6]:

$$H(x) = \frac{1+2x}{1+2x\sqrt{1-\varpi}}$$

Results and Discussion: We conducted runs with identical host grain sizes, rim thicknesses and varying iron particle sizes and abundances. Iron particle sizes ranged from 10 to 86 nm, with particle counts between 1 and 8000. Data from nine representative model runs are shown in Figure 2 and three different weight percents iron (approximately 0.01, 0.1, and 1 wt% Fe) and three different iron particle sizes (10, 20, and 40 nm). It can be seen that the primary control on the reflectance spectra in these runs was iron abundance with no observable effects due to iron particle size over this range.

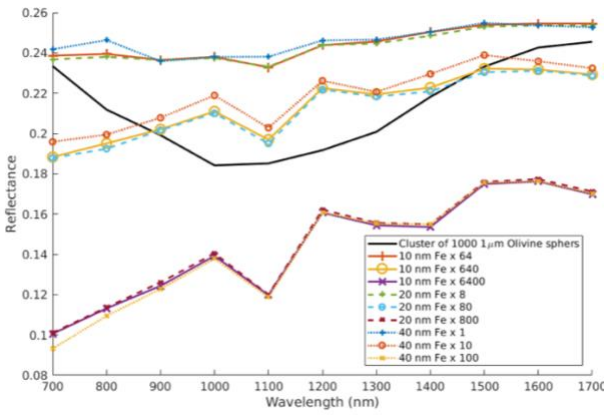

Figure 2: Comparison of 9 model runs at 3 iron sizes and 3 iron abundances. Black line is a cluster of 1000 1μm Olivine spheres.

Since both memory usage and run time correlate with the number of spheres used in a run it is difficult to directly compare runs with larger iron sizes to runs with much smaller sizes. For example, to compare a run with 10 90 nm iron particles to one with the same weight percent iron using 5 nm particles would require the use of 58320 spheres. Attempts at runs with more than ~15k spheres have not been successful. We are investigating the use of more modern light scattering codes (e.g. CELES [7]) to bypass this limitation in future experiments.

A limiting factor in the realism of our current model runs is the fact that we are attempting to model the reflectance of but a single spherical grain. Modeling clusters of 10's to 1000's of these geometrically complex grains runs afoul of the previously memory and runtime limitations due to the large number of spheres required. The local minima at 1100 and 1400 nm in the modeled spectra (Fig. 2) are likely due to the strong oscillations in scattering parameters encountered for particle/wavelength combinations in the Mie regime. A cluster of 1000 1μm olivine spheres is included in Figure 2 to show that the model can reproduce reasonable spectra in a multiple sphere case. In order to directly compare the model spectra of our space weathered grains to laboratory and remote sensing data, extension of the model to clusters of several spheres will be required. This work is currently underway (e.g. the cluster-based dense packing method [8]).

Conclusions: We show progress towards modeling more realistic grain geometries using the MSTM/Hapke hybrid method. Extension of these models to laboratory and remote sensing relevant cases is underway with results expected in the next few months. The use of GPU based codes like CELES will likely expand the utility of T-Matrix methods to more geologically relevant cases.

References:

[1] Pieters C. M. and Noble S. K. (2016) *JGR-Planet, 121,* 1865–1884. [2] Lucey P. G. and Riner M. A. (2011) *Icarus, 212,* 451-462. [3] Mackowski D. W. and Mishchenko M. I. (2011) *JQSRT, 112,* 2182–2192. [4] Mishchenko, M. I. et al. (2016) *JQSRT, 178,* 284-294. [5] Bohren C. F. and Huffman D. R. (2004) pp. 530. [6] Hapke B. (2012) pp. 513. [7] Pattelli E. A. et al. (2017), *JQSRT, 199C,* 103-110. [8] Ito et al. (2018), *in preparation.*